European Journal of Medicinal Chemistry 150 (2018) 195–205

Contents lists available at ScienceDirect

European Journal of Medicinal Chemistry

journal homepage: http://www.elsevier.com/locate/ejmech

Research paper

Anti-inflammatory hybrids of secondary amines and amide-sulfamide derivatives

Renren Bai [a, b, **], Jian Sun [a], Zhongxing Liang [b], Younghyoun Yoon [b], Eric Salgado [b], Amber Feng [b], Yoonhyeun Oum [b], Yuanyuan Xie [a], Hyunsuk Shim [b, c, d, *]

[a] College of Pharmaceutical Sciences, Zhejiang University of Technology, Hangzhou, China
[b] Department of Radiation Oncology, Emory University School of Medicine, Atlanta, Georgia, USA
[c] Winship Cancer Institute, Emory University, Atlanta, Georgia, USA
[d] Department of Radiology and Imaging Sciences, Emory University School of Medicine, Atlanta, Georgia, USA

ARTICLE INFO

Article history:
Received 12 January 2018
Received in revised form
15 February 2018
Accepted 27 February 2018
Available online 2 March 2018

Keywords:
CXCR4
Hybrids
Amide-sulfamide
Inflammation
Inflammatory cell accumulation

ABSTRACT

The CXCR4/CXCL12 chemokine axis can chemotactically accumulate inflammatory cells to local tissues and regulate the release of inflammatory factors. Developing novel CXCR4 modulators may provide a desirable strategy to control the development of inflammation. A series of novel hybrids were designed by integrating the key pharmacophores of three CXCR4 modulators. The majority of compounds displayed potent CXCR4 binding affinity. Compound **7a** exhibited 1000-fold greater affinity than AMD3100 and significantly inhibited invasion of CXCR4-positive tumor cells. Additionally, compound **7a** blocked mice ear inflammation by 67% and suppressed the accumulation of inflammatory cells in an *in vivo* mouse ear edema evaluation. Western blot analyses revealed that **7a** inhibited the CXCR4/CXCL12-mediated phosphorylation of Akt and p44 in a dose-dependent manner. Moreover, compound **7a** had no observable cytotoxicity and displayed a favorable plasma stability in our preliminary pharmacokinetic study. These results confirmed that this is a feasible method to develop CXCR4 modulators for the regulation and reduction of inflammation.

1. Introduction

Nonsteroidal anti-inflammatory drugs (NSAIDs) are among the most frequently administered drugs due to their anti-inflammatory, analgesic, and antipyretic properties [1]. Nonselective NSAIDs show unfavorable dose-dependent gastric mucosal injury side effects due to their inhibition of biosynthesis of necessary PGs by COX-1 in the stomach. Selective COX-2 inhibitors reduce the risk of gastric ulcers compared with nonselective NSAIDs, but they have been associated with an increased risk of cardiovascular side effects, including myocardial infarction, stroke, and hypertension [1-3].

The C-X-C chemokine receptor type 4 (CXCR4)/C-X-C chemokine ligand 12 (CXCL12) axis has been shown to be involved in various pathological conditions, including HIV infection, cancer and inflammation [4, 5]. Evidence has shown that the CXCR4/CXCL12 chemokine axis can chemotactically accumulate inflammatory cells (neutrophils, monocytes, and lymphocytes) to local tissues and regulate the release of inflammatory factors that cause inflammatory responses [6, 7]. Therefore, developing novel anti-inflammatory agents targeting CXCR4 may be a desirable strategy to avoid the side effects of NSAIDs.

As shown in Fig. 1, AMD3100 is the first small molecule CXCR4 antagonist to enter clinical trials for the treatment of HIV infection [8]. However, AMD3100 was not approved due to poor oral bioavailability and serious cardiotoxicity [9-11]. Taking AMD3100 as the lead compound, our research group discovered a promising bis-secondary amine drug candidate, Q-122, which is under Phase II clinical trials. Subsequent work mainly focused on modifying the two amino groups of the secondary amine structure to obtain compound RB-55 with better CXCR4 inhibitory activity, proving that the amide- sulfamide structure is a new, promising scaffold targeting CXCR4 [12].

* Corresponding author. Department of Radiation Oncology, Emory University School of Medicine, 1701 Uppergate Drive, C5018, Atlanta, GA, 30322, USA.
** Corresponding author. College of Pharmaceutical Sciences, Zhejiang University of Technology, 18 Chaowang Road, Hangzhou, Zhejiang, 310014, China.
E-mail addresses: renrenbai@zjut.edu.cn, renren.bai@emory.edu (R. Bai), hshim@emory.edu (H. Shim).

https://doi.org/10.1016/j.ejmech.2018.02.085
0223-5234/

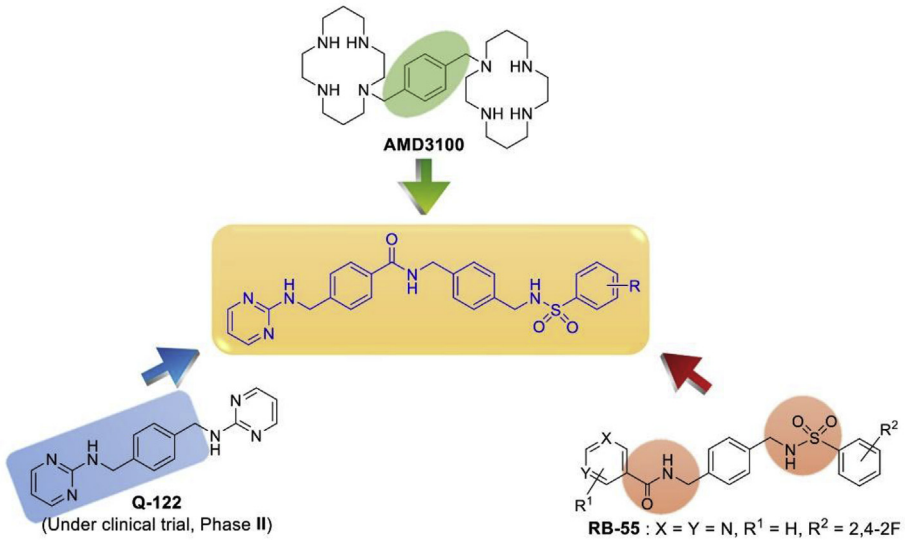

Fig. 1. Strategy for the discovery of novel amide-sulfamide anti-inflammatory agents.

The key pharmacophores of compounds AMD3100, Q-122, and RB-55 were incorporated into a single structure and a series of long-chain hybrids were designed and synthesized in the following study. The anti-CXCR4 effect, *in vivo* anti-inflammatory activity, pharmacokinetic properties, and cytotoxicity were also systematically screened.

2. Results and discussion

2.1. Chemistry

The synthetic route chosen to synthesize the targeted compounds was outlined in Scheme 1. Compounds **2a-q** were synthesized by sulfonylation of the starting material 4-(Boc-aminomethyl) benzylamine (**1**) with the corresponding sulfonyl chlorides in dichloromethane (DCM). The protective group Boc was subsequently removed in the presence of trifluoroacetic acid (TFA) producing the benzylamine intermediates **3a-q**. Compound **5** was prepared by reductive amination of another starting material terephthaldicarboxaldehyde (**4**) with 2-amino-pyrimidine. The subsequent oxidation reaction of compound **5** with Jones reagent afforded the key intermediate **6**. The final compounds **7a-q** were synthesized by the acylation of intermediate **3a-q** with acid **6**.

2.2. Primary binding affinity screening

All of the prepared compounds were first screened with a binding affinity assay as described in our previous publications [5, 12-15]. The screening protocol is a competitive CXCR4 binding assay between biotinylated TN14003, a potent CXCR4 peptidic inhibitor, and the target compounds **7a-q** at concentrations of 1, 10, 100, and 1000 nM. The effective concentration (EC) is used to measure the affinity, which is defined as the lowest concentration at which a significant reduction in the rhodamine fluorescent color is observed as compared to control (Fig. 3, without CXCR4 modulators). Thus, this initial screening is a semi-quantitative, primary screening of the level of activity, which is different from IC_{50}.

The vast majority of compounds showed comparable or even better CXCR4 binding affinity than that of AMD3100 (Table 1 and Fig. 2). Compound **7b** displayed 100-fold, and compounds **7a** and **7i** exhibited 1000-fold more potent activity than AMD3100. In terms of the benzenesulfonyl side chain, receptor affinity was obviously increased with no substitution or substitution with an electron-donating group ($-CH_3$). Moreover, when substituted with electron-withdrawing groups (-F, $-NO_2$, $-CF_3$), binding affinity remained weak, as all the ECs were no less than 1000 nM. Only 3-Cl, 4-Cl and 3,4-difluoro-substituted derivatives showed favorable activity. More importantly, when a nitrogen atom, heterocyclic, or aromatic ring were introduced to the benzenesulfonyl moiety, the affinity weakened significantly.

2.3. Matrigel invasion assay

Activation of CXCR4 through its ligand CXCL12 mediates migration and invasion. Thus, a Matrigel invasion assay was performed to probe whether the selected compounds with better binding affinities to CXCR4 can also block CXCR4/CXCR12 mediated chemotaxis and invasion [13, 15]. The target compounds and cells were added to the upper chamber of a vessel and CXCL12 was added to the lower chamber as a chemoattractant in serum-free medium. Binding of CXCR4 at the cell surface with the selected compounds would block CXCL12 chemotaxis to the cells. Therefore, MDA-MB-231 human breast cancer cells at the top chamber treated with the compounds would be inhibited to migrate from the top chamber through the Matrigel-coated filter pores to the bottom of the filter. Inhibition of cell invasion with each tested compound was calculated by comparing results to the cell invasion without treatment. The results of Matrigel invasion are summarized in Fig. 3.

All selected compounds ($EC \leq 100$ nM) effectively inhibited tumor cell invasion. Compared to the negative control group, the number of cells invading through the chamber decreased significantly, exceeding 65% inhibitory activity (Fig. 4). The compounds' anti-invasive activities was improved when sulfonamide side chain was substituted. Compounds **7d** (4-CH_3) and **7i** (3-Cl) showed the most effective anti-invasive activity, reaching 87% and 88% inhibition, respectively, which is superior to the reference drug AMD3100 (55%). The above invasion results give eloquent proof that the amide-sulfamide structure is a potent scaffold to block CXCR4 function.

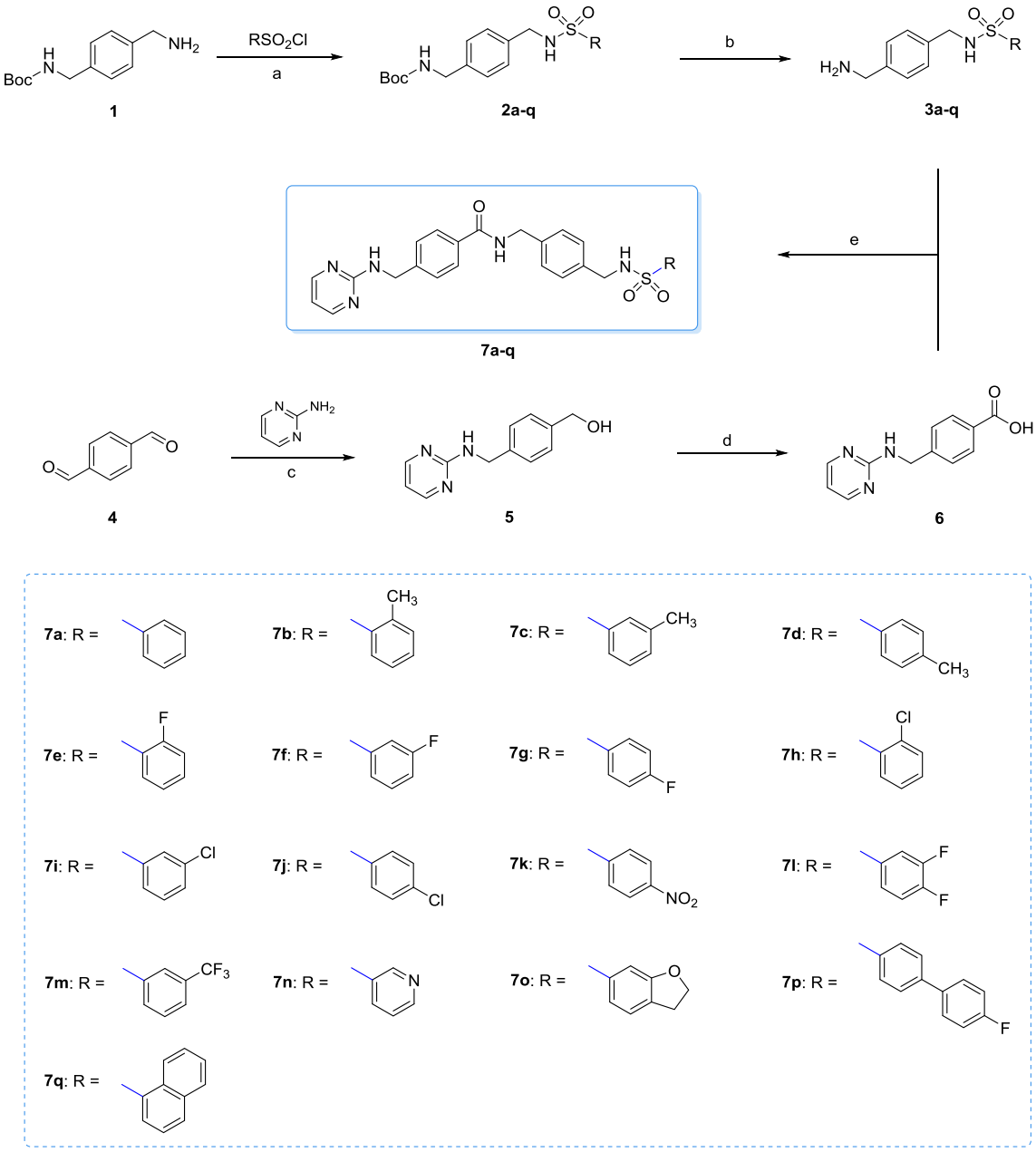

Scheme 1. Reagents and conditions: (a) DCM, TEA, ice bath to r.t., 6 h, 70–90%; (b) i. DCM, TFA, r.t., 8 h; ii. $NaHCO_3$, 90–95%; (c) $NaBH(OAc)_3$, HOAc, $ClCH_2CH_2Cl$, r.t., 12 h, 82%; (d) Jones reagent (2 M CrO_3 in aqueous H_2SO_4), ice bath, 1 h, 75%; (e) DCM, TEA, HOBT, EDCI, r.t., 16 h, 68–85%.

Table 1
Preliminary effective concentration (EC) of anti-CXCR4 compounds.

Compd	EC (nM)	Compd	EC (nM)
7a	1	**7j**	100
7b	10	**7k**	1000
7c	100	**7l**	100
7d	100	**7m**	1000
7e	1000	**7n**	>1000
7f	1000	**7o**	1000
7g	>1000	**7p**	1000
7h	1000	**7q**	1000
7i	1	AMD3100	**1000**

2.4. In vivo suppression against xylene-induced ear edema

A xylene-induced ear edema experiment was used to evaluate the *in vivo* anti-inflammatory activity of the amide-sulfamide compounds [16]. This xylene-induced ear edema model is widely used in the evaluation of inflammatory activity. The application of xylene induces the release of substance P from sensory neurons, leading to vasodilatation and plasma extravasations, which subsequently causes ear swelling in mice [17].

Compounds achieving greater than 70% inhibition in the Matrigel assay were evaluated in the ear edema test. Although AMD3100 is the best investigated small molecule CXCR4 antagonist, its bicyclam structure leads to serious toxicity in this animal model. Therefore, AMD3100 was not selected as the reference drug in this test [18]. Compounds **7d**, **7i** and **7l** were not effective in the

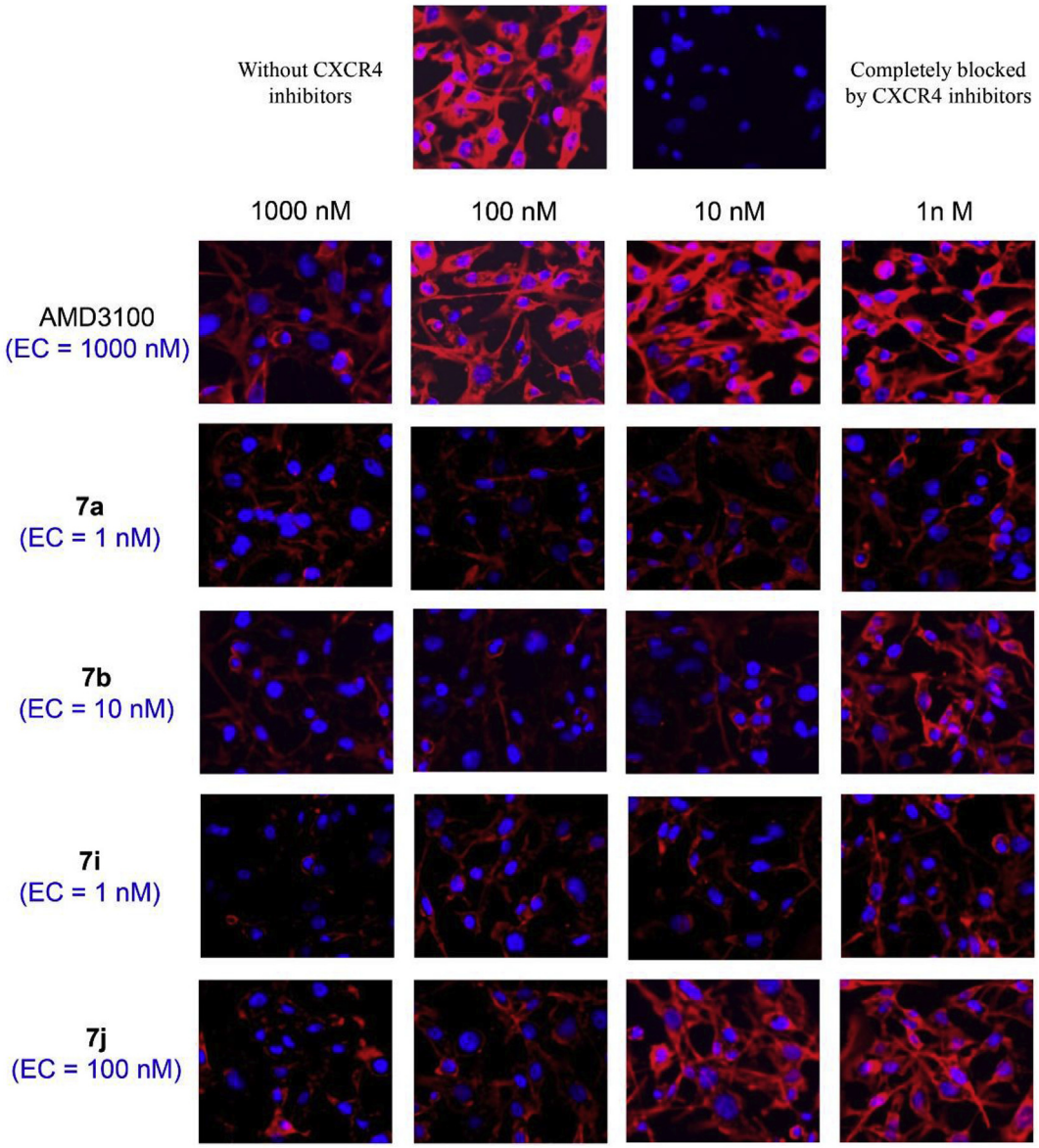

Fig. 2. Representative immunofluorescence images of competitive-binding affinity assay of three selected compounds compared to AMD3100. CXCR4 receptors on the cell surface are illustrated via the red fluorescent color in this binding affinity assay using biotinylated TN14003 that binds to CXCR4. When our test compounds are preincubated with the cells and block the binding of biotinylated TN14003, the red fluorescent color is reduced. The EC of AMD3100 was 1000 nM, while compounds **7a**, **7b**, **7i** and **7j** showed EC of only 1, 10, 1 and 100 nM, respectively. (For interpretation of the references to color in this figure legend, the reader is referred to the Web version of this article.)

treatment of inflammation (Fig. 5), while **7d** and **7j** showed moderate anti-inflammatory activity with 37% and 30% inhibition, respectively. Interestingly, the unsubstituted compound **7a** proved to demonstrate the most potent anti-inflammatory activity with 67% inhibition.

Histological analysis was performed to better study the microcosmic effect of compound **7a** on inflammatory tissues. After treatment with compound **7a**, the swollen volume and thickness of the mouse ear were significantly reduced (Fig. 6). Notably, the number of inflammatory cells in inflammatory tissues was also significantly decreased, which further propagates the anti-inflammatory mechanism whereby blocking CXCR4 could effectively inhibit the recruitment of inflammatory cells to the site of inflammation.

2.5. Evaluation of anti-CXCR4 activity of compound 7a at the molecular level

2.5.1. Compound 7a suppressed CXCL12 induced phosphorylation of Akt

Phosphoinositide 3-kinase (PI3K) activates Akt, a serine threonine kinase which plays a key role in tumor cell survival and possibly proliferation. PI3K/Akt pathways are independently involved in the proliferative signal mediated by CXCL12 [19]. Our previous results demonstrated that CXCR4/CXCL12 activation induces Akt phosphorylation, which results in tumor angiogenesis and progression of tumors by increasing expression of vascular endothelial growth factor (VEGF) [20]. The ability of **7a** to block the PI3K/Akt pathway was investigated via Western blot analysis. As

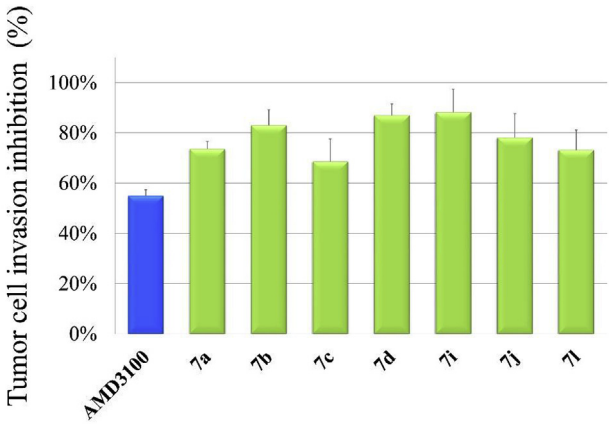

Fig. 3. Matrigel invasion assay results induced by CXCR4/CXCL12-mediated interaction using MDA-MB-231 cells. CXCL12α was added to the bottom chamber, and the compounds were added to the top chamber. After incubating for 22 h, the invading cells were fixed in methanol and stained with hematoxylin and eosin. The percent of invasion was determined by counting the stained cells.

shown in Fig. 7A, CXCR4 modulator **7a** significantly inhibited phosphorylation of Akt in a dose-dependent manner, with an active concentration of only 1 nM.

2.5.2. Compound 7a suppressed CXCL12 induced phosphorylation of p44/42

The interaction between CXCL12 and CXCR4 has also been shown to activate the extracellular signal-regulated kinase-1/2 (ERK-1/2 or also known as p44/42) in various cell types [21]. The CXCR4 inhibitory activity of compound **7a** was verified by examining its ability to block phosphorylation of p44/42. Western blot analysis proved that compound **7a** suppressed the phosphorylation of p44 effectively with a concentration of only 0.1 nM (Fig. 7B).

2.6. Molecular modeling (docking) study

To better understand the possible interaction between **7a** and CXCR4, Schrodinger Maestro Package was performed based on the available crystal structure of CXCR4 (PDB code: 3ODU [22]), the docking procedure was reported in our previous publication [13]. Fig. 8 illustrated the binding pose with the best docking score. Compound **7a** formed two hydrogen bonds with CXCR4, with the N atom in sulfonamide to Gln200 and with the N atom in amide to Glu288, respectively. In addition, the benzene ring in the amide side chain showed a π- π stacking with Trp94 and Tyr116, and the pyrimidine ring displayed another π- π stacking with Trp102 and His113. These favorable interactions are likely contributing to the binding of **7a** with CXCR4.

2.7. Preliminary pharmacokinetic study of compound 7a

The plasma stability of a drug has a significant influence on the concentration of active drug available in circulation. To determine the pharmacokinetics of this novel amide-sulfamide structure, the concentration and stability of compound **7a** in plasma were evaluated in a mouse model. The peak area of **7a** in plasma was detected by high-performance liquid chromatography (HPLC) at three time points: 5, 20 and 50 min. Generally, compound **7a** demonstrated a moderate plasma stability (Fig. 9). The approximate half-life ($t_{1/2}$) was calculated to be ~20 min. However, the basal metabolic rate per gram of body weight (the mass-specific rate) is seven times greater in mice than in humans [23]. Therefore, we inferred that $t_{1/2}$ of **7a** in human is about 2.5 h, exhibiting acceptable plasma stability.

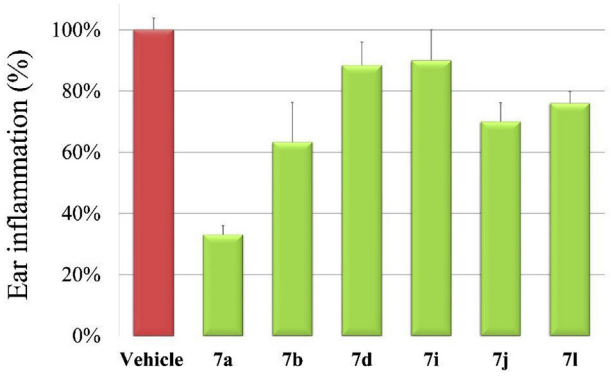

Fig. 5. In vivo anti-inflammatory test using a xylene-induced ear edema model. The right ear of each mouse was treated with 30 mL xylene. The selected compounds were administered intraperitoneally (i.p.) 30 min later at 10 mg/kg. Two hours later, one ear plug was removed from both ears and weighed to calculate the percentage of inflammatory suppression.

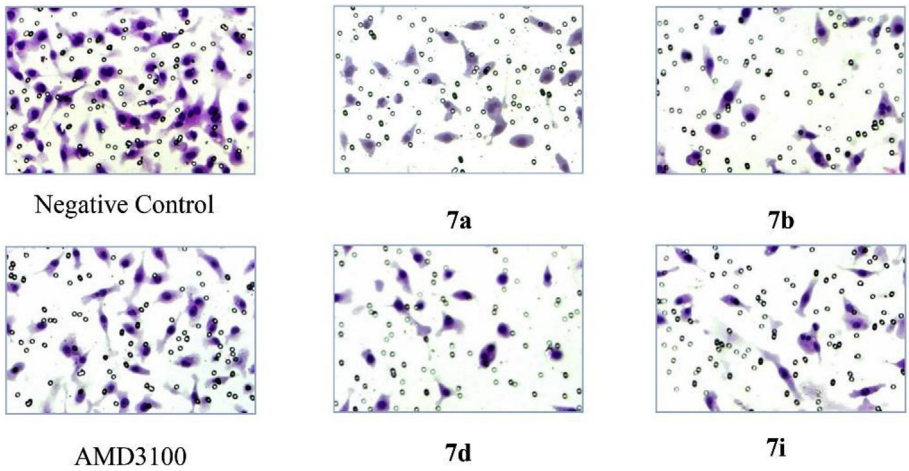

Fig. 4. Micrographs of Matrigel invasion assay induced by CXCR4/CXCL12-mediated interaction using MDA-MB-231 cells in the presence of CXCR4 modulators. The number of invading cells to the bottom chamber decreased when cells were incubated with our compounds in the top chamber.

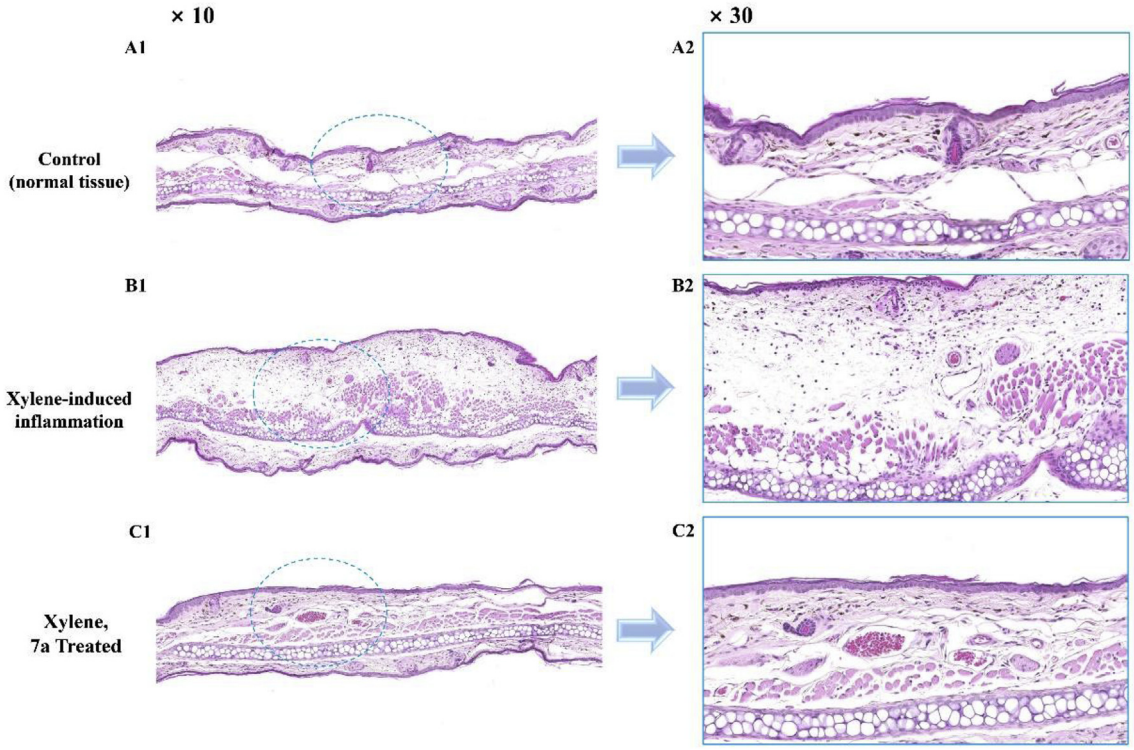

Fig. 6. Histological analysis of the anti-inflammatory activity of compound **7a**. Whole tissue slices were scanned/digitized by NanoZoomer 2.0 HT. Software NDP.view 2 was used to zoom in.

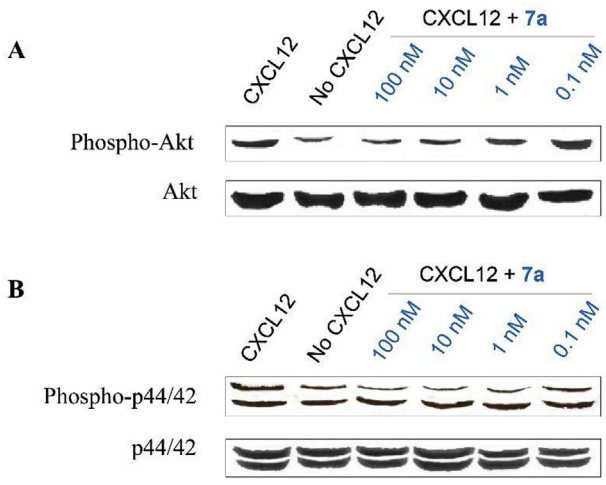

Fig. 7. Compound **7a** blocked the phosphorylation of Akt and p44/42 mediated by CXCR4/CXCL12 axis.

2.8. Cytotoxicity evaluation of compound 7a

Cytotoxic agents have the potential to cause serious destruction to healthy and normal cells. To preliminarily evaluate the safety of compound **7a**, its cytotoxicity was evaluated on two representative cell lines, MDA-MB-231 (CXCR4-positive), SKBR3 (CXCR4-positive), MCF-7 (CXCR4-positive), AC1-ExR (CXCR4-positive) and 184A1N4 (CXCR4-negative) cells, by a cell viability (MTT) assay. Of note, blocking CXCR4 should not impact adherent cell proliferation on petri dish [24]. Compound **7a** displayed potent CXCR4 binding affinity at only 1 nM, however, it did not inhibit the proliferation of MDA-MB-231and MCF-10A cells even at concentrations as high as 10 μM (Fig. 10), a 1000-fold increase to the working concentrations. Generally, **7a** had no observable cytotoxicity.

3. Conclusion

Taking the first small molecule CXCR4 inhibitor entering clinical trials, AMD3100, together with two drug candidates discovered by our research group, Q-122 and RB-55, as the lead compounds, a series of hybrids were designed by integrating the key pharmacophores of these three CXCR4 modulators. This novel amide-sulfamide scaffold maintained significant CXCR4 inhibitory capacitively, and the majority of compounds displayed potent CXCR4 binding affinity. Compounds **7a** and **7i** exhibited 1000-fold greater affinity than AMD3100. All of the compounds with favorable binding affinity significantly suppressed invasion of CXCR4 positive tumor cells. In the *in vivo* mouse ear edema evaluation, compound **7a** demonstrated the best anti-inflammatory activity, effectively blocking the aggregation of inflammatory cells to the site of inflammation. Western blot analyses revealed that **7a** inhibited the CXCR4/CXCL12-mediated phosphorylation of Akt and p44 in a dose-dependent manner. Compound **7a** also exhibited acceptable plasma stability in the preliminary pharmacokinetic study. In the cytotoxicity screening, **7a** did not inhibit the proliferation of all the tumor cell lines even at 10 μM, showing no observable cytotoxicity.

In summary, the sulfamide pharmacophore was proved to be an effective isostere of amine and amide groups because of the similarity in chemical properties. This modification is a promising strategy for the further design of CXCR4 modulators. The novel hybrids exhibited potent CXCR4 inhibitory activity both *in vitro* and *in vivo*, and showed reasonable metabolic stability with no cytotoxicity. The designed modulators could effectively inhibit the activity of CXCR4, significantly suppressing the accumulation of the

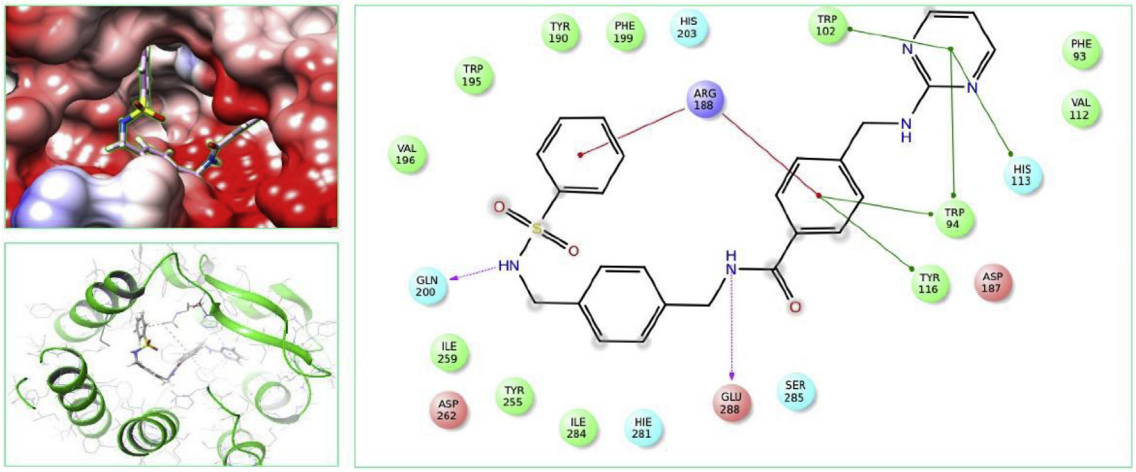

Fig. 8. A low energy predicted binding pose for compound **7a** in the CXCR4 X-ray structure.

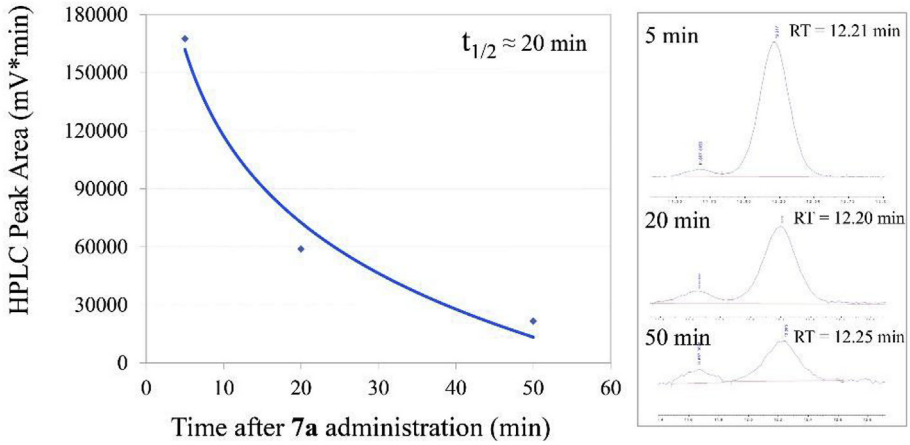

Fig. 9. The plasma stability of compound **7a** in mouse serum. Nude mice received a single dose (30 mg/kg) of compound **7a** via intravenous injection (i.v.). Blood samples were collected at 0, 5, 20 and 50 min. The blood sample was centrifuged and filtrated and analyzed by HPLC to estimate the amount of compound in serum.

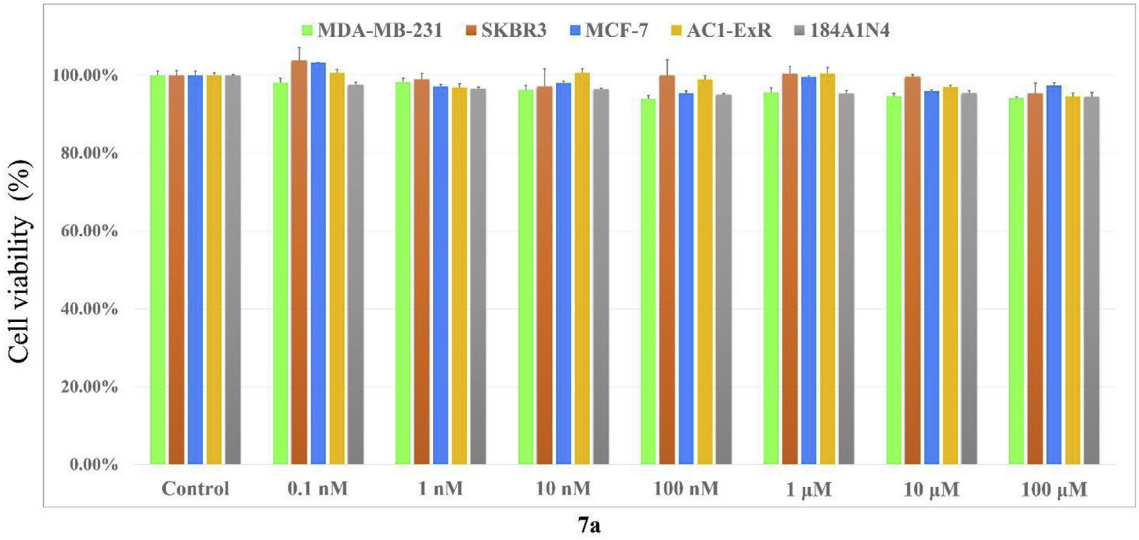

Fig. 10. Cytotoxicity evaluation of compound **7a** in MDA-MB-231, SKBR3, MCF-7, AC1-ExR and 184A1N4 cell lines. The antiproliferative activity of the compounds was determined using MTT assay. Cells were treated with Compound **7a** or vehicle control for 72 h. The results showed no statistically significant differences, which suggests that **7a** does not have antiproliferative activity.

inflammatory cells to the inflammatory sites. These results confirmed that developing CXCR4 modulators to control and reduce inflammation is a feasible and effective strategy for the treatment of inflammation.

4. Experimental section

4.1. Chemistry

4.1.1. General information

Proton and carbon NMR spectra were recorded on INOVA-400 (400 MHz) or VNMR-400 spectrometers at Emory NMR Research Center. The spectra obtained in DMSO-d6 were referenced to the residual solvent peak. Chemical shifts (δ) are reported in parts per million (ppm) relative to residual undeuterated solvent as an internal reference. Mass spectra were recorded on a JEOL spectrometer at Emory University Mass Spectrometry Center. Analytical thin layer chromatography (TLC) was performed on precoated glass backed plates from Scientific Adsorbents Incorporated (Silica Gel 60 F254; 0.25 mm thickness).

4.1.2. General procedure for synthesis of intermediate ***2a-q***

A solution of 4-(Boc-aminomethyl)benzylamine (**1**) (1.0 mmol) and TEA (3.0 mmol) in anhydrous DCM (8 mL) was cooled with an ice bath, then the corresponding sulfochloride (1.1 mmol, dissolved in 2 mL anhydrous DCM) was added dropwise. The reaction mixture was allowed to stir at 0 °C for 1 h. After removing the cooling bath, the resulting mixture was stirred for 5 h at room temperature, then diluted with saturated aqueous $NaHCO_3$ and extracted with DCM (10 mL) for three times. The combined organic layer was sequentially washed with water and brine, dried with anhydrous Na_2SO_4, and concentrated in vacuo. The crude was purified by column chromatography with DCM/methanol (150:1, v/v) to yield the product as a white solid [5].

4.1.3. General procedure for synthesis of intermediate ***3a-k***

A solution of intermediates **2** (1.0 mmol) in DCM (10 mL) was treated with trifluoroacetic acid (4 mmol) at room temperature. The resulting mixture was stirred for 8 h. The solvent was removed under reduced pressure. The residue was dissolved in saturated aqueous $NaHCO_3$ (2 mL) followed by adding more saturated aqueous $NaHCO_3$ to adjust to pH = 10. Then, the mixture was filtered and the intermediate **5** was obtained as the filter cake without further purification [5].

4.1.4. Procedure for synthesis of intermediate ***5***

To a solution of terephthaldicarboxaldehyde (**4**, 1.0 mmol) and 2-amino-pyrimidine (1 mmol) in 1,2-dichloroethane (10 mL), acetic acid (2 mmol) and 4 Å molecular sieves (0.5 g) were added, and the mixture was stirred at room temperature until 2-amino-pyrimidine completely dissolved. The resulting mixture was then treated with sodium triacetoxyborohydride (3 mmol). After being stirred for 12 h at room temperature under an argon atmosphere, the reaction was quenched by adding aqueous NaOH (10 mL, 1.0 N). The resulting mixture was extracted with ethyl acetate (3 × 10 mL), and the combined organic layers were washed with brine, dried over anhydrous Na_2SO_4, and concentrated in vacuo. The crude was purified by column chromatography with DCM/methanol (200:1, v/v) to give the product **5** as a white solid [25].

4.1.5. Procedure for synthesis of intermediate ***6***

A solution of intermediate **5** (1.0 mmol) in acetone (8 mL) was cooled with an ice bath. Jones reagent (4 mL, 2 M CrO_3 in aqueous H_2SO_4), ice bath was added dropwise. The reaction mixture was stirred at 0 °C for 30 min. Saturated aqueous $NaHCO_3$ was then added to adjust to pH = 7. Then the mixture was filtered and extracted with ethyl acetate (3 × 10 mL). The combined organic layers were washed with brine, dried over anhydrous Na_2SO_4, and concentrated in vacuo. The crude was purified by column chromatography with DCM/methanol (150:1, v/v) to give the intermediate **6** as a white solid.

4.1.6. General procedure for synthesis of target compounds ***7a-q***

To a solution of intermediate **3** (1.0 mmol), hydroxybenzotriazole (HOBT, 1.2 mmol) , 1-ethyl-3-(3-dimethylaminopropyl) carbodiimide (EDCI, 12 mmol) and TEA (3.0 mmol) in anhydrous DCM (8 mL), acid intermediate **6** (1 mmol) was added. The reaction mixture was stirred for 16 h at room temperature, then diluted with saturated aqueous $NaHCO_3$ and extracted with DCM (10 mL) three times. The combined DCM layer was sequentially washed with water and brine, dried with anhydrous Na_2SO_4, and concentrated in vacuo. The crude was purified by column chromatography with DCM/methanol to give the compound as a white solid.

*4.1.6.1. N-(4-(phenylsulfonamidomethyl)benzyl)-4-((pyrimidin-2-ylamino)methyl)benzamide (**7a**).* White solid, yield 85%, m.p. 189–191 °C. ^{1}H NMR (400 MHz, DMSO-d6) δ 8.95 (t, J = 6.0 Hz, 1H), 8.26 (d, J = 4.8 Hz, 2H), 8.12 (t, J = 6.3 Hz, 1H), 7.75–7.81 (m, 5H), 7.54–7.61 (m, 3H), 7.37 (d, J = 8.3 Hz, 2H), 7.20 (d, J = 8.3 Hz, 2H), 7.16 (d, J = 8.2 Hz, 2H), 6.58 (t, J = 4.8 Hz, 1H), 4.53 (d, J = 6.4 Hz, 2H), 4.41 (d, J = 6.0 Hz, 2H), 3.93 (d, J = 6.2 Hz, 2H). ^{13}C NMR (100 MHz, DMSO-d6) δ 166.00, 162.20, 157.96, 143.85, 140.66, 138.69, 135.99, 132.65, 132.27, 129.13, 127.51, 127.15, 127.06, 126.71, 126.40, 110.33, 45.89, 43.67, 42.25. HRMS calcd for $C_{26}H_{26}O_3N_5S$ 488.17509 [M + H]$^+$, found 488.17597.

*4.1.6.2. N-(4-(((2-methylphenyl)sulfonamido)methyl)benzyl)-4-((pyrimidin-2-ylamino)methyl)benzamide (**7b**).* White solid, yield 81%, m.p. 156–158 °C. ^{1}H NMR (400 MHz, DMSO-d6) δ 8.95 (t, J = 6.1 Hz, 1H), 8.26 (d, J = 4.7 Hz, 2H), 8.20 (s, 1H), 7.76–7.82 (m, 4H), 7.45–7.50 (m, 1H), 7.32–7.38 (m, 4H), 7.12–7.20 (m, 4H), 6.58 (t, J = 4.8 Hz, 1H), 4.54 (d, J = 6.4 Hz, 2H), 4.41 (d, J = 6.0 Hz, 2H), 3.97 (s, 2H), 2.55 (s, 3H). ^{13}C NMR (100 MHz, DMSO-d6) δ 165.98, 162.19, 157.93, 143.83, 138.88, 138.60, 136.39, 136.27, 132.65, 132.38, 132.26, 128.28, 127.41, 127.14, 126.99, 126.69, 126.10, 110.32, 45.58, 43.66, 42.24, 19.77. HRMS calcd for $C_{27}H_{28}O_3N_5S$ 502.19074 [M + H]$^+$, found 502.19088.

*4.1.6.3. N-(4-(((3-methylphenyl)sulfonamido)methyl)benzyl)-4-((pyrimidin-2-ylamino)methyl)benzamide (**7c**).* White solid, yield 80%, m.p. 126–128 °C. ^{1}H NMR (400 MHz, DMSO-d6) δ 8.95 (t, J = 6.0 Hz, 1H), 8.26 (d, J = 4.8 Hz, 2H), 8.07 (t, J = 6.2 Hz, 1H), 7.76–7.82 (m, 3H), 7.58 (d, J = 5.1 Hz, 2H), 7.36–7.47 (m, 4H), 7.21 (d, J = 8.1 Hz, 2H), 7.16 (d, J = 7.3 Hz, 2H), 6.57 (t, J = 4.8 Hz, 1H), 4.53 (d, J = 6.4 Hz, 2H), 4.41 (d, J = 5.9 Hz, 2H), 3.93 (d, J = 5.9 Hz, 2H), 2.36 (s, 3H). ^{13}C NMR (100 MHz, DMSO-d6) δ 165.99, 162.20, 157.95, 143.84, 140.58, 138.66, 136.04, 132.85, 132.65, 128.98, 127.52, 127.48, 127.15, 127.03, 126.82, 126.70, 123.56, 110.33, 45.89, 43.66, 42.25, 20.81. HRMS calcd for $C_{27}H_{28}O_3N_5S$ 502.19074 [M + H]$^+$, found 502.18989.

*4.1.6.4. N-(4-(((4-methylphenyl)sulfonamido)methyl)benzyl)-4-((pyrimidin-2-ylamino)methyl)benzamide (**7d**).* White solid, yield 83%, m.p. 194–196 °C. ^{1}H NMR (400 MHz, DMSO-d6) δ 8.96 (t, J = 6.0 Hz, 1H), 8.26 (d, J = 4.8 Hz, 2H), 8.03 (t, J = 6.3 Hz, 1H), 7.76–7.82 (m, 3H), 7.68 (d, J = 8.3 Hz, 2H), 7.37 (d, J = 8.0 Hz, 4H), 7.21 (d, J = 8.2 Hz, 2H), 7.17 (d, J = 8.2 Hz, 2H), 6.57 (t, J = 4.8 Hz, 1H), 4.53 (d, J = 6.4 Hz, 2H), 4.42 (d, J = 6.0 Hz, 2H), 3.90 (d, J = 6.3 Hz, 2H), 2.37 (s, 3H). ^{13}C NMR (100 MHz, DMSO-d6) δ 166.00, 162.20, 157.95, 143.85, 142.53, 138.68, 137.75, 136.05, 132.65, 129.56, 127.51,

127.16, 127.05, 126.71, 126.50, 110.33, 45.88, 43.67, 42.25, 20.92. HRMS calcd for $C_{27}H_{28}O_3N_5S$ 502.19074 $[M + H]^+$, found 502.19090.

*4.1.6.5. N-(4-(((2-fluorophenyl)sulfonamido)methyl)benzyl)-4-((pyrimidin-2-ylamino)methyl)benzamide (**7e**).* White solid, yield 78%, m.p. 155–157 °C. ^{1}H NMR (400 MHz, DMSO-d6) δ 8.94 (t, J = 6.0 Hz, 1H), 8.47 (s, 1H), 8.26 (d, J = 4.8 Hz, 2H), 7.71–7.82 (m, 4H), 7.58–7.64 (m, 1H), 7.29–7.38 (m, 4H), 7.18 (d, J = 8.2 Hz, 2H), 7.14 (d, J = 8.4 Hz, 2H), 6.57 (t, J = 4.7 Hz, 1H), 4.53 (d, J = 6.3 Hz, 2H), 4.39 (d, J = 6.0 Hz, 2H), 4.07 (s, 2H). ^{13}C NMR (100 MHz, DMSO-d6) δ 165.99, 162.20, 159.30, 157.96, 156.78, 143.85, 138.64, 135.97, 135.02, 134.94, 132.65, 129.48, 127.38, 127.15, 127.00, 126.71, 124.72, 124.68, 117.17, 116.96, 110.33, 45.68, 43.66, 42.23. HRMS calcd for $C_{26}H_{25}O_3N_5SF$ 506.16567 $[M + H]^+$, found 506.16474.

*4.1.6.6. N-(4-(((3-fluorophenyl)sulfonamido)methyl)benzyl)-4-((pyrimidin-2-ylamino)methyl)benzamide (**7f**).* White solid, yield 75%, m.p. 158–160 °C. ^{1}H NMR (400 MHz, DMSO-d6) δ 8.95 (t, J = 6.1 Hz, 1H), 8.26 (d, J = 4.9 Hz, 3H), 7.75–7.82 (m, 3H), 7.60–7.63 (m, 2H), 7.53–7.56 (m, 1H), 7.44–7.49 (m, 1H), 7.37 (d, J = 8.3 Hz, 2H), 7.20 (d, J = 8.3 Hz, 2H), 7.16 (d, J = 7.9 Hz, 2H), 6.58 (t, J = 4.8 Hz, 1H), 4.53 (d, J = 6.4 Hz, 2H), 4.41 (d, J = 6.0 Hz, 2H), 3.98 (d, J = 5.7 Hz, 2H). ^{13}C NMR (100 MHz, DMSO-d6) δ 165.99, 162.90, 162.20, 160.43, 157.95, 143.85, 138.78, 135.75, 132.64, 131.56, 131.48, 127.56, 127.15, 127.07, 126.70, 122.68, 122.65, 119.50, 119.30, 113.57, 113.33, 110.32, 45.91, 43.66, 42.23. HRMS calcd for $C_{26}H_{25}O_3N_5SF$ 506.16567 $[M + H]^+$, found 506.16471.

*4.1.6.7. N-(4-(((4-fluorophenyl)sulfonamido)methyl)benzyl)-4-((pyrimidin-2-ylamino)methyl)benzamide (**7g**).* White solid, yield 73%, m.p. 196–198 °C. ^{1}H NMR (400 MHz, DMSO-d6) δ 8.96 (t, J = 6.0 Hz, 1H), 8.26 (d, J = 4.8 Hz, 2H), 8.17 (s, 1H), 7.76–7.85 (m, 5H), 7.36–7.43 (m, 4H), 7.21 (d, J = 8.4 Hz, 2H), 7.16 (d, J = 8.5 Hz, 2H), 6.57 (t, J = 4.8 Hz, 1H), 4.53 (d, J = 6.4 Hz, 2H), 4.41 (d, J = 6.0 Hz, 2H), 3.95 (s, 2H). ^{13}C NMR (100 MHz, DMSO-d6) δ 166.03, 165.26, 162.76, 162.21, 157.97, 143.85, 138.75, 137.10, 135.84, 132.65, 129.49, 129.40, 127.56, 127.16, 127.07, 126.71, 116.35, 116.13, 110.34, 45.89, 43.67, 42.25. HRMS calcd for $C_{26}H_{25}O_3N_5SF$ 506.16567 $[M + H]^+$, found 506.16537.

*4.1.6.8. N-(4-(((2-chlorophenyl)sulfonamido)methyl)benzyl)-4-((pyrimidin-2-ylamino)methyl)benzamide (**7h**).* White solid, yield 80%, m.p. 170–172 °C. ^{1}H NMR (400 MHz, DMSO-d6) δ 8.93 (t, J = 6.0 Hz, 1H), 8.42 (s, 1H), 8.26 (d, J = 4.8 Hz, 2H), 7.88–7.90 (m, 1H), 7.76–7.82 (m, 3H), 7.52–7.59 (m, 2H), 7.45 (ddd, J = 7.9, 7.0, 1.7 Hz, 1H), 7.37 (d, J = 7.7 Hz, 2H), 7.15 (s, 4H), 6.58 (t, J = 4.8 Hz, 1H), 4.53 (d, J = 6.4 Hz, 2H), 4.39 (d, J = 6.0 Hz, 2H), 4.06 (s, 2H). ^{13}C NMR (100 MHz, DMSO-d6) δ 165.98, 162.20, 157.94, 143.85, 138.62, 138.24, 135.96, 133.71, 132.66, 131.58, 130.54, 130.26, 127.47, 127.41, 127.15, 126.95, 126.71, 110.33, 45.78, 43.66, 42.22. HRMS calcd for $C_{26}H_{25}O_3N_5SCl$ 522.13611 $[M + H]^+$, found 522.13623.

*4.1.6.9. N-(4-(((3-chlorophenyl)sulfonamido)methyl)benzyl)-4-((pyrimidin-2-ylamino)methyl)benzamide (**7i**).* White solid, yield 78%, m.p. 167–169 °C. ^{1}H NMR (400 MHz, DMSO-d6) δ 8.95 (t, J = 6.0 Hz, 1H), 8.28 (s, 1H), 8.26 (d, J = 4.7 Hz, 2H), 7.66–7.82 (m, 6H), 7.58 (t, J = 7.9 Hz, 1H), 7.37 (d, J = 8.2 Hz, 2H), 7.20 (d, J = 8.3 Hz, 2H), 7.15 (d, J = 8.1 Hz, 2H), 6.58 (t, J = 4.8 Hz, 1H), 4.53 (d, J = 6.4 Hz, 2H), 4.41 (d, J = 5.9 Hz, 2H), 3.98 (s, 2H). ^{13}C NMR (100 MHz, DMSO-d6) δ 165.99, 162.19, 157.94, 143.83, 142.65, 138.78, 135.65, 133.69, 132.64, 132.19, 131.15, 127.57, 127.14, 127.06, 126.69, 126.06, 125.10, 110.31, 45.91, 43.66, 42.24. HRMS calcd for $C_{26}H_{25}O_3N_5SCl$ 522.13611 $[M + H]^+$, found 522.13631.

*4.1.6.10. N-(4-(((4-chlorophenyl)sulfonamido)methyl)benzyl)-4-((pyrimidin-2-ylamino)methyl)benzamide (**7j**).* White solid, yield 75%, m.p. 196–198 °C. ^{1}H NMR (400 MHz, DMSO-d6) δ 8.95 (t, J = 6.0 Hz, 1H), 8.26 (d, J = 4.8 Hz, 2H), 8.23 (t, J = 6.2 Hz, 1H), 7.76–7.82 (m, 5H), 7.64 (d, J = 8.6 Hz, 2H), 7.37 (d, J = 8.0 Hz, 2H), 7.21 (d, J = 8.2 Hz, 2H), 7.16 (d, J = 8.2 Hz, 2H), 6.57 (t, J = 4.8 Hz, 1H), 4.53 (d, J = 6.1 Hz, 2H), 4.41 (d, J = 5.7 Hz, 2H), 3.95 (d, J = 6.2 Hz, 2H). ^{13}C NMR (100 MHz, DMSO-d6) δ 166.01, 162.20, 157.96, 143.85, 139.57, 138.78, 137.13, 135.78, 132.64, 129.25, 128.40, 127.56, 127.16, 127.07, 126.70, 110.33, 45.88, 43.66, 42.25. HRMS calcd for $C_{26}H_{25}O_3N_5SCl$ 522.13611 $[M + H]^+$, found 522.13567.

*4.1.6.11. N-(4-(((4-nitrophenyl)sulfonamido)methyl)benzyl)-4-((pyrimidin-2-ylamino)methyl)benzamide (**7k**).* White solid, yield 77%, m.p. 208–210 °C. ^{1}H NMR (400 MHz, DMSO-d6) δ 8.94 (t, J = 6.0 Hz, 1H), 8.52 (s, 1H), 8.36–8.39 (m, 2H), 8.26 (d, J = 4.8 Hz, 2H), 7.99–8.02 (m, 2H), 7.75–7.81 (m, 3H), 7.37 (d, J = 8.6 Hz, 2H), 7.20 (d, J = 8.4 Hz, 2H), 7.15 (d, J = 8.5 Hz, 2H), 6.58 (t, J = 4.8 Hz, 1H), 4.53 (d, J = 6.4 Hz, 2H), 4.39 (d, J = 6.0 Hz, 2H), 4.01 (s, 2H). ^{13}C NMR (100 MHz, DMSO-d6) δ 166.00, 162.19, 157.90, 149.42, 146.30, 143.85, 138.88, 135.53, 132.62, 128.02, 127.61, 127.14, 127.06, 126.69, 124.46, 110.32, 45.92, 43.66, 42.22. HRMS calcd for $C_{26}H_{25}O_5N_6S$ 533.16017 $[M + H]^+$, found 533.15952.

*4.1.6.12. N-(4-(((3,4-difluorophenyl)sulfonamido)methyl)benzyl)-4-((pyrimidin-2-ylamino)methyl)benzamide (**7l**).* White solid, yield 75%, m.p. 215–217 °C. ^{1}H NMR (400 MHz, DMSO-d6) δ 8.96 (t, J = 6.0 Hz, 1H), 8.20–8.31 (m, 3H), 7.76–7.82 (m, 4H), 7.62–7.66 (m, 2H), 7.37 (d, J = 8.3 Hz, 2H), 7.22 (d, J = 8.2 Hz, 2H), 7.16 (d, J = 8.1 Hz, 2H), 6.57 (t, J = 4.8 Hz, 1H), 4.54 (d, J = 6.4 Hz, 2H), 4.41 (d, J = 5.9 Hz, 2H), 3.99 (d, J = 5.8 Hz, 2H). ^{13}C NMR (100 MHz, DMSO-d6) δ 166.03, 162.21, 157.97, 153.05, 152.93, 150.54, 150.42, 150.29, 147.92, 147.79, 143.86, 138.84, 138.01, 137.97, 137.93, 135.64, 132.66, 127.63, 127.17, 127.08, 126.71, 124.33, 124.30, 124.25, 124.22, 118.62, 118.44, 116.43, 116.24, 110.33, 45.93, 43.68, 42.25. HRMS calcd for $C_{26}H_{24}O_3N_5SF_2$ 524.15624 $[M + H]^+$, found 524.15619.

*4.1.6.13. 4-((Pyrimidin-2-ylamino)methyl)-N-(4-(((3-(trifluoromethyl)phenyl)sulfonamido)methyl)benzyl)benzamide (**7m**).* White solid, yield 72%, m.p. 160–162 °C. ^{1}H NMR (400 MHz, DMSO-d6) δ 8.93 (t, J = 6.0 Hz, 1H), 8.39 (t, J = 6.0 Hz, 1H), 8.26 (d, J = 4.8 Hz, 2H), 7.95–8.04 (m, 3H), 7.75–7.81 (m, 4H), 7.37 (d, J = 8.0 Hz, 2H), 7.17 (d, J = 8.1 Hz, 2H), 7.12 (d, J = 8.3 Hz, 2H), 6.57 (t, J = 4.8 Hz, 1H), 4.53 (d, J = 6.4 Hz, 2H), 4.38 (d, J = 6.0 Hz, 2H), 4.01 (d, J = 5.9 Hz, 2H). ^{13}C NMR (100 MHz, DMSO-d6) δ 165.98, 162.20, 157.95, 143.85, 142.05, 138.79, 135.48, 132.64, 130.69, 130.46, 129.52, 128.95, 128.91, 127.58, 127.14, 127.06, 126.69, 122.98, 122.95, 110.32, 45.91, 43.66, 42.21. HRMS calcd for $C_{27}H_{25}O_3N_5SF_3$ 556.16247 $[M + H]^+$, found 556.16193.

*4.1.6.14. N-(4-((pyridine-3-sulfonamido)methyl)benzyl)-4-((pyrimidin-2-ylamino)methyl)benzamide (**7n**).* White solid, yield 68%, m.p. 213–215 °C. ^{1}H NMR (400 MHz, DMSO-d6) δ 8.95 (t, J = 6.0 Hz, 1H), 8.91 (s, 1H), 8.74 (d, J = 4.9 Hz, 1H), 8.40 (s, 1H), 8.26 (d, J = 4.8 Hz, 2H), 8.09 (ddd, J = 8.0, 2.4, 1.6 Hz, 1H), 7.82 (d, J = 8.3 Hz, 2H), 7.77 (t, J = 6.4 Hz, 1H), 7.55 (ddd, J = 8.1, 4.8, 0.8 Hz, 1H), 7.38 (d, J = 8.2 Hz, 2H), 7.19 (d, J = 8.2 Hz, 2H), 7.15 (d, J = 8.3 Hz, 2H), 6.57 (t, J = 4.8 Hz, 1H), 4.54 (d, J = 6.3 Hz, 2H), 4.40 (d, J = 5.9 Hz, 2H), 4.02 (s, 2H). ^{13}C NMR (100 MHz, DMSO-d6) δ 166.01, 162.21, 157.96, 152.77, 146.95, 143.86, 138.80, 137.18, 135.58, 134.36, 132.65, 127.59, 127.16, 127.10, 126.72, 124.12, 110.33, 45.88, 43.68, 42.24. HRMS calcd for $C_{25}H_{25}O_3N_6S$ 489.17034 $[M + H]^+$, found 489.17011.

*4.1.6.15. N-(4-(((2,3-dihydrobenzofuran)-5-sulfonamido)methyl)benzyl)-4-((pyrimidin-2-ylamino)methyl)benzamide (**7o**).*

White solid, yield 75%, m.p. 192–194 °C. ^{1}H NMR (400 MHz, DMSO-d6) δ 8.96 (t, J = 6.0 Hz, 1H), 8.26 (d, J = 4.8 Hz, 2H), 7.89 (t, J = 6.4 Hz, 1H), 7.76–7.82 (m, 3H), 7.53–7.60 (m, 2H), 7.37 (d, J = 8.3 Hz, 2H), 7.21 (d, J = 8.2 Hz, 2H), 7.16 (d, J = 8.3 Hz, 2H), 6.90 (d, J = 8.4 Hz, 1H), 6.58 (t, J = 4.8 Hz, 1H), 4.62 (t, J = 8.8 Hz, 2H), 4.53 (d, J = 6.4 Hz, 2H), 4.42 (d, J = 6.0 Hz, 2H), 3.89 (d, J = 6.3 Hz, 2H), 3.21 (t, J = 8.8 Hz, 2H). ^{13}C NMR (100 MHz, DMSO-d6) δ 166.01, 162.75, 162.20, 157.96, 143.85, 138.61, 136.12, 132.64, 132.24, 128.60, 127.74, 127.54, 127.15, 126.99, 126.70, 123.93, 110.33, 108.91, 72.07, 45.90, 43.66, 42.24, 28.44. HRMS calcd for $C_{28}H_{28}O_4N_5$ 530.18565 $[M + H]^+$, found 530.18544.

*4.1.6.16. N-(4-(((4′-fluoro-[1,1′-biphenyl])-4-sulfonamido)methyl) benzyl)-4-((pyrimidin-2-ylamino)methyl)benzamide (**7p**).* White solid, yield 80%, m.p. 172–174 °C. ^{1}H NMR (400 MHz, DMSO-d6) δ 8.96 (t, J = 6.0 Hz, 1H), 8.26 (d, J = 4.8 Hz, 2H), 8.18 (t, J = 6.3 Hz, 1H), 7.86 (s, 4H), 7.76–7.81 (m, 5H), 7.32–7.38 (m, 4H), 7.22 (d, J = 8.4 Hz, 2H), 7.19 (d, J = 8.4 Hz, 2H), 6.57 (t, J = 4.8 Hz, 1H), 4.53 (d, J = 6.4 Hz, 2H), 4.41 (d, J = 5.9 Hz, 2H), 3.97 (d, J = 6.2 Hz, 2H). ^{13}C NMR (100 MHz, DMSO-d6) δ 166.02, 163.63, 162.20, 161.19, 157.96, 143.85, 142.77, 139.40, 138.72, 136.01, 135.05, 135.02, 132.65, 129.23, 129.14, 127.55, 127.32, 127.15, 127.07, 126.70, 116.05, 115.84, 110.33, 45.91, 43.67, 42.26. HRMS calcd for $C_{32}H_{29}O_3N_5FS$ 582.19697 $[M + H]^+$, found 582.19752.

*4.1.6.17. N-(4-((naphthalene-1-sulfonamido)methyl)benzyl)-4-((pyrimidin-2-ylamino)methyl)benzamide (**7q**).* White solid, yield 82%, m.p. 159–161 °C. ^{1}H NMR (400 MHz, DMSO-d6) δ 8.92 (t, J = 6.0 Hz, 1H), 8.66 (d, J = 9.0 Hz, 1H), 8.50 (t, J = 6.1 Hz, 1H), 8.26 (d, J = 4.8 Hz, 2H), 8.17 (d, J = 8.2 Hz, 1H), 8.04–8.11 (m, 2H), 7.76–7.81 (m, 3H), 7.58–7.72 (m, 3H), 7.37 (d, J = 8.1 Hz, 2H), 7.11 (d, J = 8.3 Hz, 2H), 7.07 (d, J = 8.3 Hz, 2H), 6.57 (t, J = 4.8 Hz, 1H), 4.53 (d, J = 6.4 Hz, 2H), 4.37 (d, J = 5.9 Hz, 2H), 3.98 (d, J = 6.1 Hz, 2H). ^{13}C NMR (100 MHz, DMSO-d6) δ 165.97, 162.20, 157.96, 143.84, 138.56, 136.08, 135.76, 133.81, 133.59, 132.66, 128.86, 128.35, 127.74, 127.49, 127.35, 127.15, 126.90, 126.75, 126.70, 124.72, 124.44, 110.33, 45.69, 43.67, 42.21. HRMS calcd for $C_{30}H_{28}O_3N_5S$ 538.19074 $[M + H]^+$, found 538.19150.

4.2. Primary binding affinity screening

For binding affinity assay, 2×10^4 MDA-MB-231 cells in 300 μL of cell culture medium were seeded in an 8-well slide chamber two days before the experiments were conducted. Various concentrations of different compounds (1, 10, 100, or 1000 nM) were added to the separate wells and incubated for 10 min at room temperature, and then the cells were fixed in 4% ice-cold paraformaldehyde. The cells were rehydrated in phosphate-buffered saline (PBS). The slides were subsequently incubated for 30 min at room temperature with 0.05 μg/mL biotinylated TN14003, washed three times with PBS, and incubated in streptavidin-rhodamine (1:150 dilution; Jackson ImmunoResearch Laboratories, West Grove, PA) for 30 min at room temperature. Finally, the slides were washed with PBS and mounted in an anti-fade mounting solution (Molecular Probes, Eugene, OR), and the samples were analyzed on a Nikon Eclipse E800 microscope [13, 15, 25].

4.3. Matrigel invasion assay

Matrigel invasion assay was performed by using a Matrigel invasion chamber from Corning Biocoat (Bedford, MA). CXCL12α (200 ng/mL; R & D Systems, Minneapolis, MN) was added to the bottom chamber to induce the invasion of MDA-MB-231 cells through the Matrigel. The selected compounds (100 nM) or AMD3100 were added to the cells before the cells were seeded in the top chamber. The Matrigel invasion chamber was incubated for 22 h in a humidified cell culture incubator. First, non-invading cells were removed from the top of the Matrigel with a cotton-tipped swab. Invading cells on the filter at the bottom of the Matrigel were fixed in methanol and stained with hematoxylin and eosin (H & E). The percent of invasion was determined by counting the H&E stained cells [13, 15].

4.4. Xylene-induced ear inflammation suppression test

Five mice per group were used to determine the effect of the CXCR4 modulators. The inner and outer surfaces of the right ear of each mouse were treated with a total 30 μL of xylene for the induction of ear edema, whereas the left ear surfaces were treated with 30 μL of saline, which was used as a non-inflammation control. The selected compounds were dissolved in 10% DMSO and 90% of 45% (2-hydroxypropyl)-β-cyclodextrin (CD) in PBS. 30 min after the application of xylene, 14 selected compounds were administered intraperitoneally (i.p.) at 10 mg/kg. Control animals received corresponding i.p. injections of the vehicle. The animals were sacrificed 2 h later, and two ear plugs (7 mm in diameter) were removed from both the treated ear and the untreated ears. Weights of treated and untreated ear plugs were measured. The difference in weight of the two ear plugs was taken as a measure of edematous response. The inflammation-suppression percentage was calculated by comparing the drug-treated group to the control group [16].

4.5. Western blot analysis

Forty micrograms of protein were separated by SDS-PAGE and transferred to a PVDF membrane (Bio-Rad, Hercules, CA, USA). The membrane was blocked for 30 min in a blocking solution (5% milk in Trisbuffered saline containing 0.1% Tween-20) and incubated overnight at 4 °C using monoclonal rabbit anti-phospho-Akt (Ser473) antibody (Cat No., 9271)/monoclonal rabbit anti-Akt (pan) antibody (cat No., 4691) or monoclonal rabbit anti-phospho-p44/42 MAPK (Thr202/Tyr204) antibody (cat No., 4376)/ monoclonal rabbit anti-p44/42 MAPK antibody (cat No., 4695) at 1:500 in blocking solution. All antibodies were purchased from Cell Signaling Technology (Danvers, USA). The membrane was incubated for 1 h with goat anti-rabbit IgG (H + L)-HRP conjugated secondary antibody at 1:10000 (Cat No. 1706515; Bio-rad, Hercules, USA) after washing. Enzyme-linked chemiluminescence was performed to detect hybridized protein bands.

4.6. Preliminary pharmacokinetic study of compound 7a

Nude mice with body weight about 20 g were used in the PK study. The mice were anaesthetized with Ketamine hydrochloride (90 mg/kg) and Xylazine (4.5 mg/kg). Compound **7a** was dissolved in 10% DMSO and 90% of 45% (2-hydroxypropyl)-β-cyclodextrin (CD) in PBS. The mice were warmed by the heat lamp for 2 min and then received a single dose (30 mg/kg) of compound **7a** via intravenous injection (i.v.). Blood samples (100 μL) were collected at 0, 5, 20 and 50 min post-dose from orbital venous sinus with heparinized capillary tubes (I.D. 1.1–1.2 mm). After collection, the blood sample was centrifuged at 13000 g for 4 min at 4 °C. The supernatant was then filtrated by microcon centrifugal filter (10000 NMWL) at 13000 g for 30 min at 4 °C. The filtrate was frozen at −80 °C until HPLC analysis. The HPLC analysis of the blood sample was performed on a C18 column (250*4.6 mm). Acetonitrile (0.1%TFA)-Water (0.1%TFA) (50:50, V/V) was applied as the mobile phase and the detective wavelength was set at 254 nm.

4.7. Preliminary cytotoxicity study of compound 7a (MTT assay)

The antiproliferative activity of the compounds was determined using MTT assay. Cells were seeded in 96-well microculture plates at 3000 cells/well in 100 μL of medium and incubated for 24 h at 37 °C in CO_2 incubator. Following the incubation for 24 h, these cells were treated with Compound **7a** for 24 h at 37 °C. Finally, 20 μL of CellTiter 96AQ reagent (Promega, Madison, WI) was added into each well and incubated for an additional 2 h, and the absorbance at 490 nm was measured.

Acknowledgments

This study was financially supported by a research grant from NIH NCI (R01 CA165306).

Appendix A. Supplementary data

Supplementary data related to this article can be found at https://doi.org/10.1016/j.ejmech.2018.02.085.

References

[1] G. Bozimowski, A review of nonsteroidal anti-inflammatory drugs, AANA journal 83 (2015) 425–433.
[2] C. Pereira-Leite, C. Nunes, S.K. Jamal, I.M. Cuccovia, S. Reis, Nonsteroidal anti-inflammatory therapy: a journey toward safety, Medicinal research reviews 37 (2017) 802–859.
[3] S.K. Suthar, M. Sharma, Recent developments in chimeric NSAIDs as safer anti-inflammatory agents, Medicinal research reviews 35 (2015) 341–407.
[4] H. Zhang, D. Kang, B. Huang, N. Liu, F. Zhao, P. Zhan, X. Liu, Discovery of non-peptide small molecular CXCR4 antagonists as anti-HIV agents: recent advances and future opportunities, European journal of medicinal chemistry 114 (2016) 65–78.
[5] R. Bai, Z. Liang, Y. Yoon, E. Salgado, A. Feng, S. Gurbani, H. Shim, Novel anti-inflammatory agents targeting CXCR4: design, synthesis, biological evaluation and preliminary pharmacokinetic study, European journal of medicinal chemistry 136 (2017) 360–371.
[6] H. Shi, R. Lu, S. Wang, H. Chen, F. Wang, K. Liu, Effects of SDF-1/CXCR4 on acute lung injury induced by cardiopulmonary bypass, Inflammation 40 (2017) 937–945.
[7] R.C. Furze, S.M. Rankin, Neutrophil mobilization and clearance in the bone marrow, Immunology 125 (2008) 281–288.
[8] G.A. Donzella, D. Schols, S.W. Lin, J.A. Este, K.A. Nagashima, P.J. Maddon, G.P. Allaway, T.P. Sakmar, G. Henson, E. De Clercq, J.P. Moore, AMD3100, a small molecule inhibitor of HIV-1 entry via the CXCR4 co-receptor, Nature medicine 4 (1998) 72–77.
[9] M. Lefrancois, M.R. Lefebvre, G. Saint-Onge, P.E. Boulais, S. Lamothe, R. Leduc, P. Lavigne, N. Heveker, E. Escher, Agonists for the chemokine receptor CXCR4, ACS medicinal chemistry letters 2 (2011) 597–602.
[10] A. Scozzafava, A. Mastrolorenzo, C.T. Supuran, Non-peptidic chemokine receptors antagonists as emerging anti-HIV agents, Journal of enzyme inhibition and medicinal chemistry 17 (2002) 69–76.
[11] C.W. Hendrix, C. Flexner, R.T. MacFarland, C. Giandomenico, E.J. Fuchs, E. Redpath, G. Bridger, G.W. Henson, Pharmacokinetics and safety of AMD-3100, a novel antagonist of the CXCR-4 chemokine receptor, in human volunteers, Antimicrobial agents and chemotherapy 44 (2000) 1667–1673.
[12] R. Bai, Q. Shi, Z. Liang, Y. Yoon, Y. Han, A. Feng, S. Liu, Y. Oum, C.C. Yun, H. Shim, Development of CXCR4 modulators by virtual HTS of a novel amide-sulfamide compound library, European journal of medicinal chemistry 126 (2017) 464–475.
[13] R. Bai, Z. Liang, Y. Yoon, S. Liu, T. Gaines, Y. Oum, Q. Shi, S.R. Mooring, H. Shim, Symmetrical bis-tertiary amines as novel CXCR4 inhibitors, European journal of medicinal chemistry 118 (2016) 340–350.
[14] T. Gaines, D. Camp, R. Bai, Z. Liang, Y. Yoon, H. Shim, S.R. Mooring, Synthesis and evaluation of 2,5 and 2,6 pyridine-based CXCR4 inhibitors, Bioorganic & medicinal chemistry 24 (2016) 5052–5060.
[15] S.R. Mooring, J. Liu, Z. Liang, J. Ahn, S. Hong, Y. Yoon, J.P. Snyder, H. Shim, Benzenesulfonamides: a unique class of chemokine receptor type 4 inhibitors, ChemMedChem 8 (2013) 622–632.
[16] K. Lalrinzuali, M. Vabeiryureilai, G.C. Jagetia, Investigation of the anti-inflammatory and analgesic activities of ethanol extract of stem bark of sonapatha oroxylum indicum in vivo, Int J Inflam 2016 (2016), 8247014.
[17] M. Eddouks, D. Chattopadhyay, N.A. Zeggwagh, Animal models as tools to investigate antidiabetic and anti-inflammatory plants, Evid Based Complement Alternat Med 2012 (2012) 142087.
[18] H.K. Shu, Y. Yoon, S. Hong, K. Xu, H. Gao, C. Hao, E. Torres-Gonzalez, C. Nayra, M. Rojas, H. Shim, Inhibition of the CXCL12/CXCR4-axis as preventive therapy for radiation-induced pulmonary fibrosis, PLoS One 8 (2013), e79768.
[19] S. Barbero, R. Bonavia, A. Bajetto, C. Porcile, P. Pirani, J.L. Ravetti, G.L. Zona, R. Spaziante, T. Florio, G. Schettini, Stromal cell-derived factor 1alpha stimulates human glioblastoma cell growth through the activation of both extracellular signal-regulated kinases 1/2 and Akt, Cancer Res 63 (2003) 1969–1974.
[20] Z. Liang, J. Brooks, M. Willard, K. Liang, Y. Yoon, S. Kang, H. Shim, CXCR4/CXCL12 axis promotes VEGF-mediated tumor angiogenesis through Akt signaling pathway, Biochem Biophys Res Commun 359 (2007) 716–722.
[21] E. Zuccolo, C.A. Di Buduo, F. Lodola, S. Orecchioni, G. Scarpellino, D.A. Kheder, V. Poletto, G. Guerra, F. Bertolini, A. Balduini, V. Rosti, F. Moccia, Stromal Cell-derived Factor-1alpha Promotes Endothelial colony Forming Cell Migration through the Ca2+-dependent Activation of the Extracellular Signal-regulated Kinase 1/2 and Phosphoinositide 3-kinase/AKT Pathways, Stem Cells and Development, 2017.
[22] B. Wu, E.Y. Chien, C.D. Mol, G. Fenalti, W. Liu, V. Katritch, R. Abagyan, A. Brooun, P. Wells, F.C. Bi, D.J. Hamel, P. Kuhn, T.M. Handel, V. Cherezov, R.C. Stevens, Structures of the CXCR4 chemokine GPCR with small-molecule and cyclic peptide antagonists, Science 330 (2010) 1066–1071. New York, N.Y.
[23] L. Demetrius, Of Mice and Men, when it Comes to Studying Ageing and the Means to Slow it Down, Mice Are Not Just Small Humans, 6, 2005, pp. S39–S44.
[24] Z. Liang, T. Wu, H. Lou, X. Yu, R.S. Taichman, S.K. Lau, S. Nie, J. Umbreit, H. Shim, Inhibition of breast cancer metastasis by selective synthetic polypeptide against CXCR4, Cancer Res 64 (2004) 4302–4308.
[25] A. Zhu, W. Zhan, Z. Liang, Y. Yoon, H. Yang, H.E. Grossniklaus, J. Xu, M. Rojas, M. Lockwood, J.P. Snyder, D.C. Liotta, H. Shim, Dipyrimidine amines: a novel class of chemokine receptor type 4 antagonists with high specificity, J Med Chem 53 (2010) 8556–8568.